Journal of Ceramic Processing Research. Vol. 9, No. 2, pp. 172~175 (2008)

J O U R N A L O F
Ceramic Processing Research

Pyroelectric properties of BSCT thick films for uncooled infrared detectors

Hyun-Ji Noh[a], Sung-Gap Lee[a,*] and Young-Hie Lee[b]

[a]*Dept. of Ceramic Engineering, Eng. Res. Insti., I-Cube Center, Gyeongsang National University, Gyeongnam, 660-701, South Korea*
[b]*Dept. of Electronic Materials Engineering, Kwangwoon University, Seoul 139-701, South Korea*

Ferroelectric $(Ba_{0.54}Sr_{0.36}Ca_{0.10})TiO_3$(BSCT) thick films were fabricated by a screen printing method on high purity alumina substrates, and the structural and electrical properties with the variation of the number of screen-printings were examined for uncooled infrared detector applications. The lattice constant of BSCT thick films was 0.3952 nm and there is no dependence on the variation of thickness. The thickness of thick films obtained by one screen-printing was approximately 7 μm. The relative dielectric constant increased and the Curie temperature decreased with an increase in the number of screen printings, an increase in film thickness. The pyroelectric coefficient of the 9-printed BSCT thick films was 270×10^{-9} Ccm^{-2}K^{-1} at the Curie temperature. The figures of merit, F_V for the voltage responsivity and F_D for the specific detectivity, of the 9-printed BSCT thick films were 3.1×10^{-11} Ccm/K and 1.7×10^{-9} Ccm/K, respectively.

Key words: Screen-printing, Thick Films, Ferroelectric, Perovskite, Pyroelectric properties

Introduction

Uncooled infrared (IR) detectors have been rapidly developed over the past several years. In particular, IR detectors operating at room temperature are attractive to many civilian and military applications, such as night vision, surveillance, detection of gas leakages, fire rescue operations, manufacturing quality control, early fire detection and guidance, missile tracking and interception [1-3]. There are basically two types of IR detectors: photon and thermal types. Generally, photon types are preferred primarily due to their superior sensitivity and resolution. However, the sensor must be cryogenically cooled down during operation to maintain high sensitivity. Uncooled thermal detectors have attracted much attention because they operate at room temperature. These devices offer the advantage of low cost fabrication and a broadband of 8-12 μm operation coupled with a performance adequate for many applications, especially in the consumer field [4].

Ferroelectric $BaTiO_3$ system ceramics have received much attention for their possible application in the dynamic random access memories, tunable microwave devices and various types of transducers due to their high spontaneous polarization and dielectric properties [5,6]. Generally, many studies to date on $BaTiO_3$ system ceramics have been focused on dielectric and positive temperature coefficient (PTC) thermistor applications, so that only a few studies on the pyroelectric properties of these materials have been carried out. However, $BaTiO_3$ ceramics, partially substituted with Sr^{+2} ions at the A-sites (Ba^{+2} ions), showed the good pyroelectric properties for application in IR detectors [7].

In this study, $BaTiO_3$ powders, partially substituted with Sr^{+2} and Ca^{+2} ions at the A-sites (Ba^{+2} ions) were prepared by a sol-gel method in order to decrease the phase transition temperature and to improve the pyroelectric properties at around 20°C. $(Ba,Sr,Ca)TiO_3$ thick films were fabricated by a screen printing method on alumina substrates. The structural and electrical properties were examined for uncooled infrared detector applications.

Experimental

The chemical composition of the specimens is given by the formula $(Ba_{0.54}Sr_{0.36}Ca_{0.1})TiO_3$ (BSCT). This BSCT composition gave a transition temperature below room temperature. BSCT powders, starting with a mixture of Ba acetate [$Ba(CH_3COO)_2$], Sr acetate hemihydrate [$Sr(CH_3COO)_2 \cdot 0.5H_2O$], Ca acetate monohydrate [$Ca(CH_3COO)_2 \cdot H_2O$] and Ti isopropoxide {$Ti(OCH(CH_3)_2)_4$}, were prepared by a sol-gel method. Acetic acid (CH_3COOH) and 2-methoxyethanol ($CH_3OCH_2CH_2OH$) were used as solvents. Ba, Sr and Ca acetate were dissolved in acetic acid, and then the solution was heated to evaporate the water. After cooling, Ti isopropoxide, dissolved in 2-methoxyethanol, was added to the solution. The mixed solution was refluxed and then 2-methoxyethanol and water were added to the solution for stabilization and hydrolysis, respectively. The powder precursors were dried and then calcined at 900°C for 2 h in a high purity alumina crucible and ground by planetary ball milling for 24 h.

*Corresponding author:
Tel : +82-55-7515333
Fax: +82-55-7515333
E-mail: lsgap@gnu.ac.kr

The screen-printable pastes were prepared by kneading the ground BSCT powder with 30wt% of organic binder (Ferro Co. B75001) in a non-bubbling kneader (NBK-1, Kyoto Electro.). High purity alumina was used as a substrate. The bottom electrodes were prepared by screen printing Pt paste and firing at 1450°C for 20minutes. After screen printing the BSCT paste using a 200 mesh screen mask, printed films were dried at 80°C for 30minutes. These processes from printing to drying were repeated from 6 times to 9 times. The thick films were sintered at 1420°C for 2h in air. The upper electrodes were fabricated by screen printing with Ag paste.

X-ray diffraction (XRD) and scanning electron microscopy (SEM) were introduced in order to analyze the crystallinity and the microstructure of BSCT specimens, respectively. The dielectric properties were measured using an impedance analyzer (HP 4194). The pyroelectric current i_p was the average value of those measured repeatedly using a digital electrometer (Keithley 6514) at a constant rate of temperature change of 5 Kminute^{-1}. After measuring i_p, the pyroelectric coefficient p was derived from:

$$p = i_p/[(dT/dt) \cdot S] \ [C/cm^2 \cdot K] \quad (1)$$

where, i_p is the pyroelectric current [A], S is the electrode area [cm^2], T is the absolute temperature [K], t is the time [s] and dT/dt is 0.083 (K/s).

Discussion and Results

Fig. 1 shows the differential thermal analysis (DTA) and the thermogravimetry (TG) curves of the dried $(Ba_{0.54}Sr_{0.36}Ca_{0.1})TiO_3$ powders. The weight loss of dried powders derived from the sol-gel method was about 42% at 1000°C, as determined by the TG curve. An endothermic peak due to the evaporation of absorbed water and solvent were observed in the temperature range of 100°C to 350°C. Due to the combustion of organic residues, exothermic peaks were observed at around 400°C. The weight loss in the temperature range of 600°C to 700°C was attributed to the decomposition of barium carbonate, which was formed during heating [8]. An exothermic peak was observed at around 660°C due to the formation of the polycrystalline perovskite phase.

The X-ray diffraction analysis of BSCT thick films with the number of screen-printings showed the typical cubic polycrystalline structure and a single phase of BSCT which was found to be in good agreement with the crystallinity and no-second phase, as shown in Fig. 2. The lattice constant of BSCT thick films was 0.3952 nm and there is no dependence on the variation of thickness.

Fig. 3 shows the surface and the cross-sectional SEM micrographs of the BSCT thick films with the number of screen-printings. BSCT thick films 6-times screen-printed had a porous structure with a large pore size, as shown in Fig. 3(a) and (c). However, the 9-times screen-printed thick films showed a small pore size and much dense microstructure. The average grain size of all thick films was about 1.6 μm. All BSCT thick films

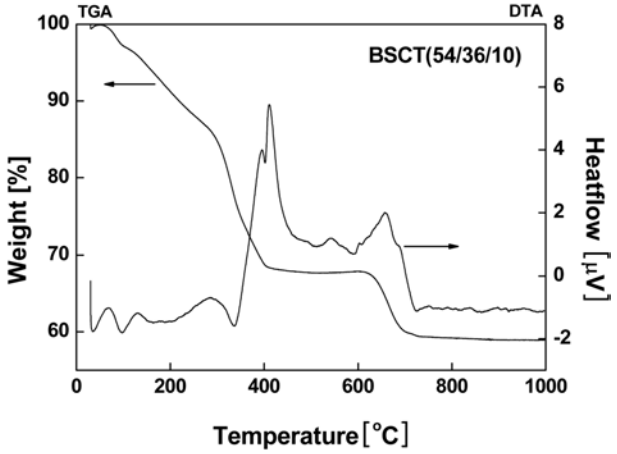

Fig. 1. DTA/TGA curves of the dried BSCT powders.

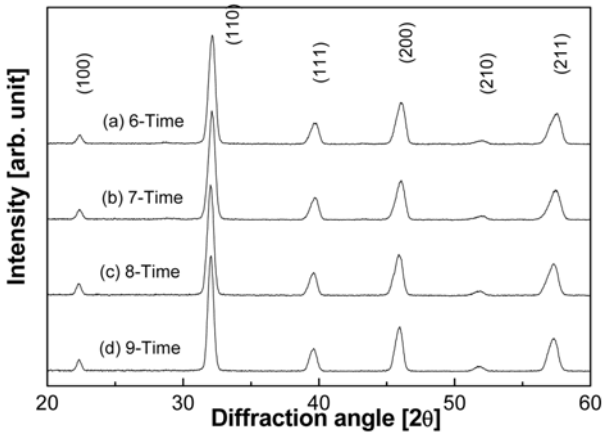

Fig. 2. X-ray diffraction patterns of the BSCT thick films with the number of screen printings.

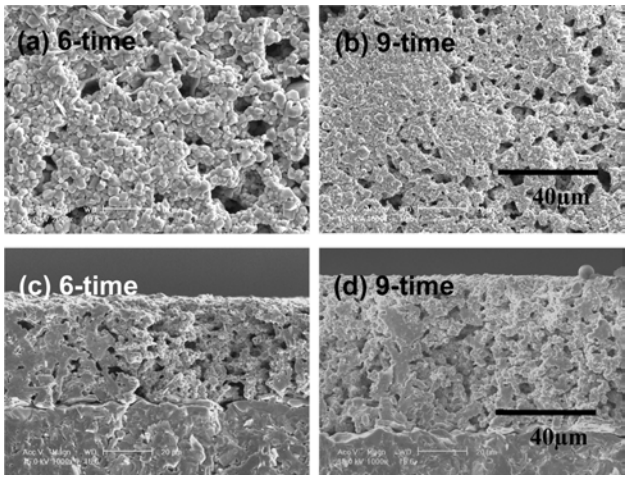

Fig. 3. Surface and cross-sectional SEM micrographs of BSCT thick films with the number of screen printings.

adhered to the Pt/alumina substrate without cracking and exfoliation, and the thicknesses of 6-times and 9-times screen-printed thick films were approximately 40 μm and 60 μm, respectively.

Fig. 4 shows the relative dielectric constant and dielectric loss of BSCT thick films as a function of temperature at 100 Hz. The Curie temperature of BSCT specimens decreased with a decrease in the Ba/(Sr+Ca) ratio. For substitution Sr^{2+}-Ba^{2+}, the bonding force between the A-site ion and the oxygen ion of ABO_3 perovskite structure becomes stronger because the radius of the Ba^{2+} ion (0.135 nm) is larger than that of the Sr^{2+} ion (0.113 nm): the bonding force Ti-O(Sr), therefore, becomes weaker than the Ti-O(Ba) bond. The weakening of the Ti-O bond leads to a weaker distortion of the octahedron and brings about a decrease in the c/a ratio, thus inducing a drop in the Curie temperature [9]. The relative dielectric constant increased and the Curie temperature decreased with an increase in the number of screen-printings, an increase in the film thickness. These properties can be explained by the increment of densification and the reduction of the stress induced between the thicker film and substrate. The relative dielectric constant at 20°C and Curie temperature of the 9-printed thick films were 2729 and 17°C, respectively. The 6-printed BSCT thick films showed high dielectric loss properties due to the large pores, as shown in Fig. 3. However, the dielectric loss of the thick films screen-printed more than 7-times was independent of the number of screen-printings and all BSCT thick films showed good values less than 0.5% at higher than 20°C.

Fig. 5 shows the pyroelectric coefficient of BSCT thick films with the variation of the number of screen-printings and temperature. The 9-printed BSCT thick film showed the maximum value of 270×10^{-9} C/cm^{2}K at its Curie temperature because of the increment of densification and the large variation of the dielectric constant-temperature curve.

Generally, the pyroelectric performance of the ferroelectric ceramics can be measured in terms of the figures of merit (FOM), *e.g.*:

$$F_V = p/(c_v K) \text{ and } F_D = p/[c_v(K \tan d)^{1/2}] \quad (2)$$

where, p = pyroelectric coefficient, c_v = volume specific heat (= 3.2 J/cm^{3}K)[10], K = dielectric constant, and tand δ = dielectric loss. F_V and F_D are the relevant FOMs when the device noises are dominated by the readout amplifier and the Johnson noise in the element, respectively [11].

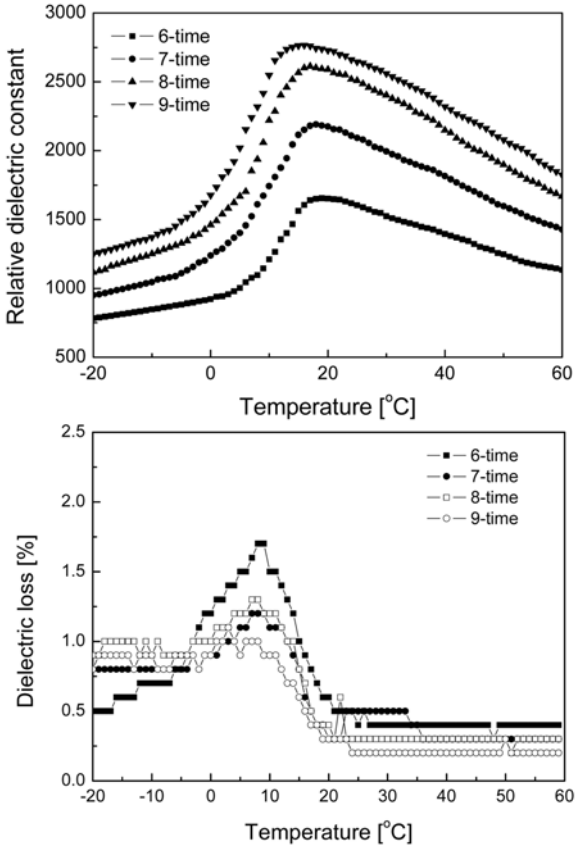

Fig. 4. Relative dielectric constant and dielectric loss at 100 Hz of BSCT thick films as a function of the temperature.

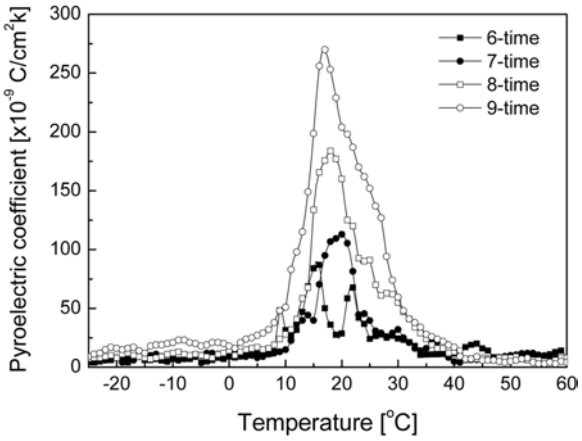

Fig. 5. Pyroelectric coefficient of BSCT thick films as a function of the temperature.

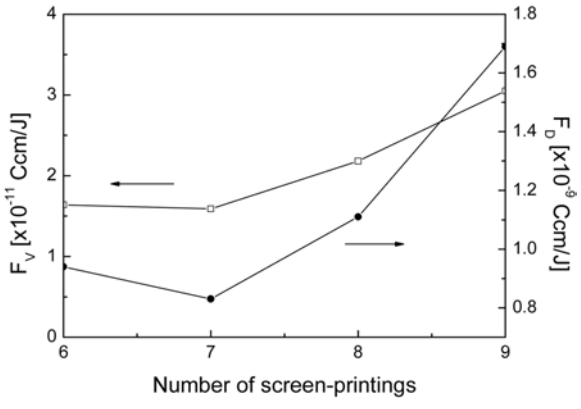

Fig. 6. Pyroelectric figures of merit, F_V and F_D, of BSCT thick films with the number of screen printings.

Fig. 6 shows the F_V and the F_D of the BSCT thick films as function of the number of the screen-printings at the Curie temperature. The F_V changes slightly with an increase in the number of screen-printings due to an increase in the pyroelectric coefficient, as shown in Fig. 5. For the 9-printed BSCT thick films, F_V and F_D have their highest values of 3.1×10^{-11} Ccm/K and 1.7×10^{-9} Ccm/K, respectively.

Conclusions

In this research, $(Ba_{0.54}Sr_{0.36}Ca_{0.10})TiO_3$ powders, prepared using a sol-gel method, were mixed with an organic binder, and BSCT thick films were fabricated by screen-printing techniques. The XRD, result from the BSCT thick films showed the typical cubic XRD patterns of a perovskite polycrystalline structure. The relative dielectric constant increased and dielectric loss decreased with an increase in the number of screen-printings, the values of the 9-printed BSCT thick films were 2729, 0.25% at 20°C, respectively. The average grain size of all thick films was about 1.6 μm and the thicknesses of 9-times screen printed thick films was about 60 μm. The pyroelectric coefficient of the 9-printed BSCT thick films was 270×10^{-9} $Ccm^{-2}K^{-1}$ at the Curie temperature. The 9-printed BSCT thick films showed good figures of merit characteristics due to their good dielectric and pyroelectric properties.

Acknowledgement

This work has been supported by KESRI (R-2005-7-094), which is funded by MOCIE (Ministry of Commerce, Industry and Energy).

References

1. C. M. Wang, Y. C. Chen, M. S. Lee, C. C. Chiou, Y. T. Huang, Jpn. J. Appl. Phys. 38[5](1991) 2831-2834.
2. G. D. Cicco, B. Morten, D. Dalmonego, M. Prudenziati, Sensors and Actuators A:Physical 76[1](1999) 409-415.
3. T. Futakuchi, Z. K. Tanino, H. Sawasaki, M. Adachi, A. Kawabaa, Jpn. J. Appl. Phys. 36[9](1997) 5981-5983.
4. R.W. Whatmore, P. C. Osbond, N. M. Shorrocks, Ferroelectrics 76 (1987) 351-367.
5. P. Chen, H. Miki, Y. Shimamoto, Y. Matsui, M. Hiratani, Y. Fujisaki, Jpn. J. Appl. Phys. 37[9] (1998) 5112-5117.
6. L.C. Sengupta, S. Stowell, E. Ngo, M.E. O'Day, R. Lancio, Integrated Ferroelectric, 8[1&2] (1995) 77-88.
7. D. S. Kang, M.S. Han, S.G. Lee, S.H. Song, J. of Eur. Ceram. Soc. 23[3](2003) 515-518.
8. T. Hayashi, H. Shinozaki and K. Sasaki, Jpn. J. Appl. Phys. 37[9](1998) 5232-5236.
9. J. Ravez, C.R. Acad. Sci. Paris, Serie Iic, Chimie/Chemistry, 3 (2000) p. 267.
10. B. M. Kulwicki, A. Amin, H. R. Beratan, C. M. Hanson, Proc. 8th Int. Symp. Appl,. Ferroelectrics (Greenville, SC, Aug. 31, 1992), IEEE, 1993, p. 1.
11. R. W. Whatmore, O. Molten, C. P. Shaw, J. Eur. Ceram. Soc. 23[5](2003) 721-728.